Efficient Prediction and Uncertainty Propagation of Correlated Loads

I. Tartaruga[1], J.E. Cooper[2] and M. Lowenberg[3]
Dept of Aerospace Engineering, University of Bristol, Bristol, BS8 1TR, UK

S. Coggon[4]
Airbus Operations Ltd, Filton, Bristol, BS99 7AR, UK

and

Y. Lemmens[5]
Siemens,3001 Leuven, Belgium

Aircraft structural design is influenced by the static and dynamic loads resulting from flight manoeuvres, gust/turbulence encounters and ground manoeuvres; thus the identification of such loads is crucial for the development and the structural analysis of an aircraft and requires the solution of the aeroelastic dynamic responses. Numerical aeroelastic models are used to predict a large number (1000s) of "Interesting Quantities" (IQs). For an Aircraft design, the IQs related to the worst case are significant, but their identification implies a significant computational effort. Of particular interest are the so-called correlated loads, where coincident values of pairs of IQs are plotted against each other. This paper demonstrates how to reduce the computational burden to determine the behaviour of the correlated loads envelopes with little reduction in the accuracy, and also to quantify the effects of uncertainty, for a range of different parameters. The methodology is evaluated on a numerical aeroelastic wing model of a civil jet airliner.

Nomenclature

$\boldsymbol{A}$	=	matrix to which the SVD is applied
D	=	number of sampling points
M	=	number of case loads
$\boldsymbol{U}$	=	matrix of the right singular vector
$\boldsymbol{V}$	=	matrix of the left singular vector
$\boldsymbol{\Sigma}$	=	diagonal matrix of the singular values
λ	=	singular value
N	=	number of time steps
S	=	number of stations of interest
$f(\boldsymbol{x})$	=	Kriging regression function
H	=	gust gradient
L_g	=	gust length, $2 \cdot H$
I, J	=	inertia moments of the bar element
s	=	distance penetrated into the gust
U	=	gust velocity

[1] PhD reasearcher, Dept of Aerospace Engineering, E-mail: irene.tartaruga@bristol.ac.uk.
[2] Royal Academy of Engineering Airbus Sir George White Professor of Aerospace Engineering, Dept of Aerospace Engineering, E-mail: j.e.cooper@bristol.ac.uk.
[3] Professor of Flight Dynamics, Department of Aerospace Engineering, E-mail: M.Lowenberg@bristol.ac.uk.
[4] Ground Loads Modeling Expert, E-mail: Simon.Coggon@airbus.com.
[5] Sr Project Leader RTD, E-mail: yves.lemmens@siemens.com.

$\boldsymbol{x}$ = vector of the input parameters
x_{ij} = element of a matrix
$\hat{y}(\boldsymbol{x})$ = estimated function, predictor in the surrogate model theory
y = actual function
z_{ij} = element of a normalized matrix
$Z(\boldsymbol{x})$ = Kriging regression function
μ = mean
σ = root mean square
ψ = basis function
θ and p = free parameters used in the Kriging methods

I. Introduction

THE design and development of an aircraft are tasks that require multidisciplinary analyses. Central constraints in the design process are the loads and the aeroelastic response characterizing the structure during its operating life. The external and internal loads have a strong impact upon structural design, aerodynamic characteristics, flight control system and control surface design, weight and performance. In this regard, the development of methods that provide fast, but accurate, prediction of loads will enable a quicker determination of the critical loads cases and also permit more design configurations to be considered.

Of particular interest is the identification of those loads that lead to the most extreme stress levels for a specific design. This aim is achieved by applying a large number of loads cases due to dynamic gusts and manoeuvres to detailed aeroelastic models[1-3] for a range of different Interesting Quantities (IQs) e.g. bending moments, shear forces, etc. Table 1 shows an estimate of the number of conditions that are typically required in the analysis of a large civil aircraft. Even with simplistic models of aircraft behaviour being used, this is an unfeasible number of separate simulations; however, engineering experience is used to identify the most likely critical loads conditions, meaning that approximately 100,000 simulations are required for conventional aircraft configurations. Furthermore, these analyses have to be repeated every time that there is an update in the aircraft structure. Within the modern civil airframe industry, each of these loads calculation cycles takes a considerable time.

50	Flight points (altitude and speed)
100	Mass cases (loaded weight and weight distribution)
10	Control surface configurations
50	Manoeuvres and gusts (gradient lengths)
4	Control laws
10,000,000	TOTAL NUMBER OF CASES REQUIRED

Table 1. Estimate of Load Cases Required[4].

Previous work in the FFAST FP7 project[4-7] has investigated the use of several surrogate modeling (also known as surrogate models) and optimization methods for fast and efficient prediction of the worst case gust loads for each IQ. It has been shown that savings in computational time can be made without sacrificing accuracy. Further studies considered the effect of changes to the actual aircraft structure as part of the evolving design process[6] using reanalysis methods.

In the previous work, the worst case gust loads were found for each IQ independently. However, it is essential to take into account the effect of correlation between the IQs, such as bending moment and torque, since the combination of IQs values and not only the maximum (in magnitude) of each of the IQs can provide a critical condition.

This analysis is possible by considering the so-called "potato" plots which are obtained by considering the correlated loads, a set of loads that are consistent across the aircraft in time. To construct these plots, relevant pairs of IQs are extracted at the same instant of time for all the load cases and, after having plotted these responses, the envelope of all the points is computed.[6] The critical cases can be found as the vertices of the global convex hull.

All of the critical load conditions for an aircraft could be identified if a method were developed that is able to capture:

1. The behaviour of the convex hull
2. The correlated loads at different stations at the same critical case load
3. The critical case loads and relative instant for all the desired stations

One may carry out Monte Carlo Simulation (MCS) directly running the numerical model to calculate all the time histories of IQs at any possible points in the space of input parameters; however, MCS is computationally expensive.

[6] The envelope can be determined using a Convex Hull Algorithm, such as the MATLAB® function "convhull".

For individual IQs, the use of surrogate models can be used to decrease the computational time without losing accuracy[4-7].

A further area where there has been little work in the aircraft loads is that of uncertainty quantification to predict the effect of variations in the structure (manufacturing tolerance and material properties) and the aerodynamics (atmospheric variations and forces resulting from geometric variations). Research in this field has been recently increased since the industrial companies themselves are aware that a deterministic approach, with the application of safety factor, involves an over or under designed system. Most work in this area related to aeroelastic effects[8-14] has been concentrated upon the effect of uncertainties on critical phenomena such as flutter and divergence rather than loads. A very preliminary investigation relating to the uncertainty quantification of correlated gust envelopes was undertaken by Khodaparast. H H et al.[7] using a simple 2 DOF aeroelastic model and exploiting the Polynomial Chaos Expansion (PCE)[8-10]. The PCE technique is one of several methods to quantify the uncertainty for which a statistical description of the inputs is known and it is often applied to aleatory uncertainties in the aeronautical field. For example, uncertainties in the properties of composite-structures[9-11] and in the stiffness of the structure[8-14] have been studied to understand their effect on the flutter velocity[6,11-13,15-16].

In this work, a methodology will be described that satisfies the above critical load condition requirements, and can be achieved with reduced computational cost. The investigation will consider prediction of the changes in the structural parameters of the wings, using the Singular Value Decomposition (SVD) and a range of different Surrogate Models, such as Kriging and Neural Networks, and the Latin Hypercube Sampling (LHS) method.

Uncertainty Quantification (UQ) has been applied in order to efficiently determine the effects of design change (engine mass and engine pylon stiffness). Thanks to the developed technique, it is possible to use a probabilistic approach to propagate the effect of uncertainties (e.g. PDF, CDF and quantiles) in the design parameters on each individual IQ and also the "potato" plots resulting from families of "1 – cosine" (1MC) gusts. The approach is demonstrated by considering IQs (bending moments and torques) arising from loads due to families of 1MC gusts acting upon a wing / pylon / engine structure of a typical civil jet aircraft model..

II. Aircraft and Load Models

A Aircraft Model

The aircraft model used is a representative civil jet airliner, the FFAST model[6], whose nominal weights and main dimensions are reported in Table 2 . The structural model of the aircraft was a beam-stick model with lumped masses. (Fig. 1) and the aerodynamics modelled using the *Doublet-Lattice Method* (DLM)[17].

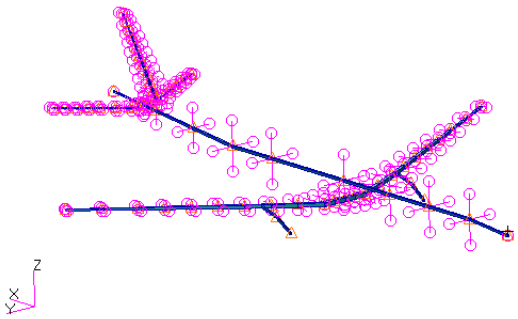

Figure 1. Structural Model of the aircraft.

Weights		Dimension	
MTOW	23110^3kg	Wing span	57.83
MLW	18710^3kg	Mean chord	6.07 m
OEW	12310^3kg		
MZFW	17510^3kg	**Other**	
Max Payload	51.7 10^3kg	Cruise Speed	241.7m/s
Total fuel	110 10^3kg	Max operating altitude	12500 m
Mean Engine Weight	8694.3 kg		
Mean Wing Weight	3.2 10^4kg		

Table 2. Main weights and dimensions of the FFAST Model.

B Gust Model

Turbulence is an unfortunate feature of air travel regularly encountered by aircraft which occurs due to the movement of the air, causing dynamic response of the aircraft. The turbulence induces a variation in the effective incidence of the aerodynamic surfaces (related to wings, tails, control surfaces etc…) which changes the lift and drag forces acting on the aircraft structure.

Suitable models are needed for design purposes in order to determine the gust and turbulence loads, some of which are likely to be the critical cases. Different approaches[1] have been developed since the 1970s; a historical perspective is given in Fung (1969), Hoblit (1988), Flomenholft (1994), Fuller (1995) and Bisplinghof et al. (1996). The latest requirements for civil aircraft are found in the EASA Certification Specifications (CS-25) and Federal Aviation

Regulations (FAR-25)[18]. In these requirements two types of gust and turbulence have to be considered, to represent the conditions that are met in flight:

- *Discrete gusts*, where the gust velocity is assumed to vary in a deterministic way. The most common shape, used in the CS/FAR, is the called '1-cosine' (1MC) shape.
- *Continuous turbulence*, where the gust velocity is considered to vary randomly. In this work, the 1MC gusts will be considered.

In this work, 1MC gusts were considered (Fig. 2) specified in the CS/FAR[2,18] as

$$U = \frac{U_{ds}}{2}\left[1 - \cos\left(\frac{\pi s}{H}\right)\right] \qquad \text{for } 0 \le s \le 2H \qquad (1)$$

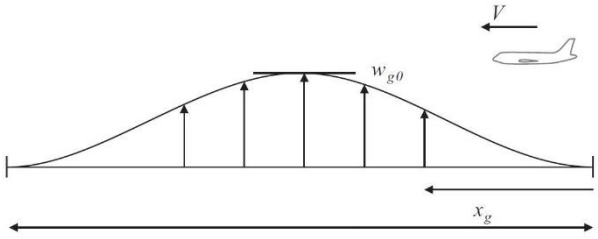

Figure 2. Discrete '1-cosine' gust[1].

and, as the aim is to determine the critical response for each IQ, a sufficient number of gust gradient distances H in the range 9 to 107 meters must be investigated (gust length = 2 x gust gradient).

Ten different gust gradients[7] were considered as input cases across the entire range of gust lengths.

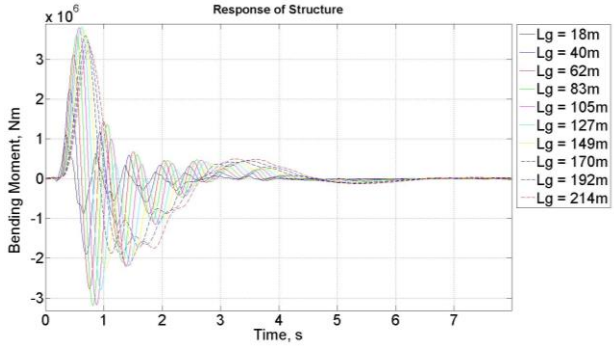

Figure 3. IQ Time Histories for Different Gust Lengths

the SVD is adopted to accomplish the feature selection[19] and surrogate models are considered rather than running the numerical model. In particular, the surrogate models are trained and validated using the Latin Hypercube Sampling (LHS) method [20] .

As well as determining the maximum and minimum response for each IQ[4-7, 31], it is also of interest to determine "correlated loads" as the critical stresses / strains will be dependent upon a combination of Moment, Axial, Shear and Torque (MAST) loads. The correlated responses (or correlated loads) (Fig. 3), can be plotted against each other, as shown in Fig. 4, determining the so called "potato" plots. Once the load is selected, the outlying points of a convex hull are used to define the critical solicitations at each station of the structure.

III. Methodology

The aim of the present paper is to present a new methodology to efficiently predict correlated quantities, and hence the convex hulls in the presence of design parameter variations without sacrificing accuracy, and then to propagate the uncertainties. Here, variations in the structure parameters of the model civil jet airliner were considered; namely the mass, flexural and torsional stiffness of the wings, the mass of the engines and the stiffness of the pylons. The uncertainties considered here are related to the mass of engine and the stiffness of the pylon; both are epistemic and aleatory uncertainties since both the lack of knowledge and uncertainties inherent in the problem can cause them. In order to speed up the process,

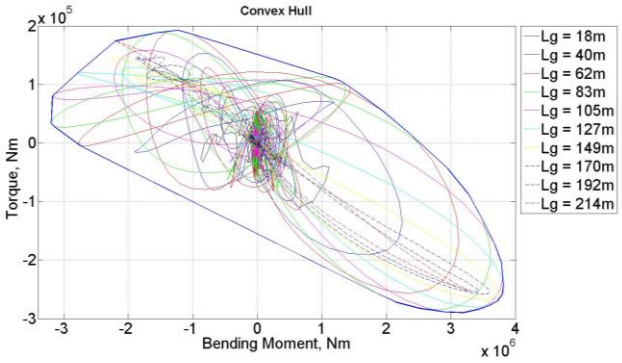

Figure 4. 2D Correlated Loads for Different Gust Lengths

[7] The gust lengths considered in the present problem are (in metres): [18, 40, 62, 83, 105, 127, 149, 170, 192, 214]

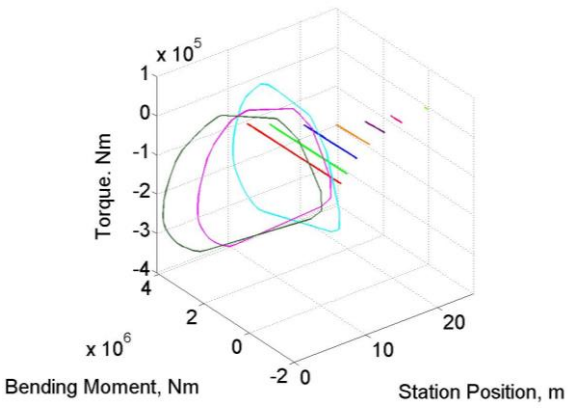

Figure 5. Correlated Loads Envelope obtained at the wing root and its behaviour along the wing considering a family of ten 1MC gusts.

In the present paper, a convex hull in terms of the Bending Moment and the Torque of the wings has been considered. Note that both the number and the time instants characterizing a critical case usually change as parameters vary or different stations are considered.

In this regard, Fig. 5 presents the variation of the shape and area of the correlated loads plots along one wing (10 stations have been considered from the root to the tip of the wing). Moreover, considering families of 1MC gusts, the outlying points at each single station are commonly related to different gust wavelength Lg.

The proposed methodology can be divided in three parts as summarized in Fig. 6.

1. Application of SVD
2. Surrogate Model Selection
3. Uncertainty Quantification

In what follows each part of the methodology will be detailed presentated.

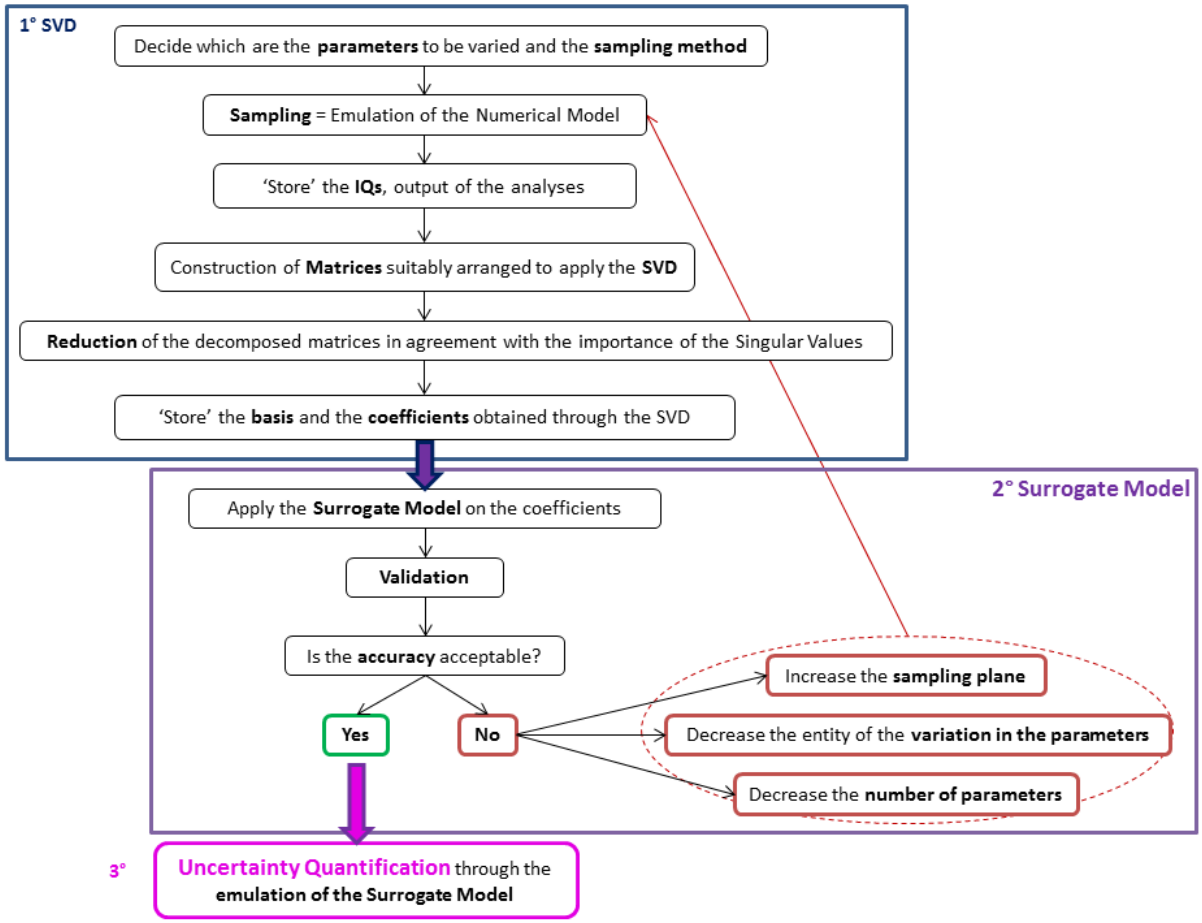

Figure 6. Flow chart of the Methodology.

A Application of Singular Value Decomposition

The Singular Value Decomposition (SVD) is a mathematical operation to decompose a rectangular matrix, used to analyze and simplify problems in several fields. In linear algebra it is commonly used to obtain ranks, kernels, norms and solution of simultaneous equations for over-determined systems. Moreover, it is very useful in data analysis, for instance noise removal, visualization and dimensionality reduction.

The SVD is defined as[22]: *for every matrix* $\boldsymbol{A} \in \mathbb{R}^{m\times n}$ *there exist two orthogonal matrixes* $\boldsymbol{U} \in \mathbb{R}^{m\times m}$ *and* $\boldsymbol{V} \in \mathbb{R}^{n\times n}$ *and a diagonal matrix* $\in \mathbb{R}^{m\times n}$ *, whose diagonal contains the non-negative singular values* $\lambda_1 \geq \lambda_2 \geq \cdots \geq \lambda_{min\{n,m\}} \geq 0$ *, such that* $\boldsymbol{A}$ *can be decomposed as* $\boldsymbol{A} = \boldsymbol{U\Sigma V^T}$.

In order to reduce the dimension of a problem, $\boldsymbol{A_T}$, a *truncated* SVD can be considered. It is the matrix obtained considering only the columns of $\boldsymbol{U}$ and $\boldsymbol{V}$ (i.e. the *singular vectors*) related to the *k highest* singular values; usually the non-zero singular values are chosen although this can be sometimes difficult to do in practice, and therefore the most significant terms are retained. Although several methods have been investigated (*Guttman-Kaiser criterion*, *Captured Energy*, *Cattell's Scree test*) a general approach that automatically identifies the correct rank for truncated SVD has not been yet identified, and this is mainly due to the inability on real data sets to determine where the cut-off needs to be made.

In the aeronautics field, the SVD has been used for over 30 years, applied to a range of different purposes including system identification and modal analysis. Recently, Sarkar et al.[23] have developed, demonstrated and tested a SVD-based method for symbolic design optimization problem reformulation. Such a method has been applied to Hydraulic Cylinder Design and Aircraft Concept Sizing. Armstrong[24] used such a technique both to accomplish a down-selection procedure in terms of loads, identifying a suitable set of unit loads, and also to predict the response of a structure faster.

In this new methodology the SVD is adopted for feature extraction by fixing a basis and then using other coefficients to obtain the required information. The basis is given by the product of the diagonal matrix and the matrix containing the *right singular vectors*, namely $\boldsymbol{\Sigma}_k \boldsymbol{V}_k^T \in \mathbb{R}^{k\times m}$; the coefficients that vary with respect to the design parameters are the terms in the matrix of the *left singular vectors* ($\boldsymbol{U}_k$).

Initially the parameters to be varied are decided upon, and then a sampling method is selected. Two kinds of sampling points must be determined:

1. those that will be used to train the surrogate model (so called training points)
2. those that will be considered to validate the surrogate model

The numerical model has to be run at each sampling point. If the objective is to determine the critical 1D or 2D points, then only the first two cycles of the dominant mode need to be saved and the rest of the time history can be ignored. Having saved all of the required time responses, a matrix is constructed for each IQ. For example here, the Bending Moment and the Torque at 10 stations along each wing have been selected as IQs. The matrix, defined for each IQ, has as many rows as the number of parameter variations (e.g. engine mass, pylon stiffness) (D) and as many columns as the product of the number of time steps in each response (N), the number of configurations/ environmental conditions (e.g. case loads as gust lengths, altitudes) (M) and the number of stations of interest (S). Thus, the dimensions of each matrix are (D) x (NxMxS). The structure of the matrix is shown in Table 3.

	Station 1			**…**	**Station S**		
	Case Load 1	**…**	**Case Load M**	**…**	**Case Load 1**	**…**	**Case Load M**
Training	**Time (1:N)**	**…**	**Time (1:N)**	**…**	**Time (1:N)**	**…**	**Time (1:N)**
1	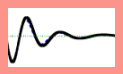	…	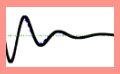	…	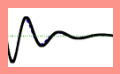	…	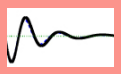
…	…	…	…	…	…	…	…
D	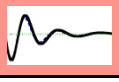	…	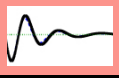	…	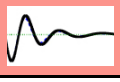	…	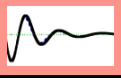

Table 3. Matrix constructed for each IQ, to be decomposed through the SVD

The SVD is applied to each IQ matrix so that both a basis and set of coefficients can be related to each IQ. The basis for the computations is given by $\boldsymbol{\Sigma}_{\mathrm{k}}\boldsymbol{V}_k^T$, whose dimensions are (K) x (N x M x S), where K is the number of singular values that are retained, and this is assumed not to change throughout the design space. Consequently, the time histories of each IQ at different stations, for different configurations/ environmental conditions and for a specific i-th sampling point can be simply identified by multiplying the respective row vector of coefficient $(\boldsymbol{U}_{\mathrm{k}})_i$ by the fixed basis $\boldsymbol{\Sigma}_{\mathrm{k}}\boldsymbol{V}_k^T$.

B Surrogate Model Selection

After having identified these matrices, surrogate models of each of the K columns in the **U** matrix can be developed in order to enable both prediction and UQ of the correlated IQs.

The use of surrogate models presents a key opportunity in all branches of physics and engineering to efficiently explore the design space and also the effects of uncertainty. In fact, surrogate models are able to simulate complex problems guaranteeing the required accuracy without incurring too much computation, which characterizes most of the current emulators since the significant improvements in computational fluid and structural modelling over the last two decades. Surrogate models[25] are developed using sampled data obtained by running simulations at particular training points in the region of interest. They have been applied in numerous fields, for instance for design space exploration, visualization, prototyping and sensitivity analysis[26], to deal with noisy or missing data, and also for data mining i.e. to understand which data/variables have the most impact[25]. Approaches often used are *Kriging* based methods, *Neural Network*, *Regression Tree* and *Polynomial Radial Basis Functions*.

There are several different *Kriging* surrogate models and the difference is related to the particular form of the regression function.[25 -30] The main ones are:

- *Simple Kriging*, which assumes the regression function to be a known constant.
- *Ordinary Kriging* that considers a constant but unknown regression function ($f(\boldsymbol{x}) = \hat{\mu}$).
- *Blind Kriging*, which assumes the regression function to be a completely unknown function. This function is identified using a Bayesian variable selection technique.

The latter method, *Blind Kriging*, is preferable to the *Ordinary Kriging* which suffers:

1. Reduced performance in the presence of strong trends[31].
2. Lack of direct information about the effects of the factors, just looking at the predictor (it is necessary to use a sensitivity analysis such as the functional analysis of the variance)
3. Lack of robustness in the presence of misspecification in the correlation parameters, which are difficult to be exactly evaluated.

Polynomial Radial Basis Functions are regression models in which the selected basis is polynomial[25] and *Neural Network* (NN) can be considered as a generalization of the Radial Basis Fuction, in fact the latter is a neural network with a single hidden Layer[17].

Moreover, the NN includes a huge set of approaces that can be classified as follows:

- Feedforward Networks (MLP/Radial Basis Function)
- Recurrent Networks (Elman Networks)
- Cellular Networks (SOM, Self Organising Map)

Finally, *Regression Tree* can be described in a series of logical if-then conditions (tree nodes) and is attractive since its simplicity and the lack in assuming linear and/or monotonic link-function between output and input variables[32]. The aforementioned surrogate models have been compared in order to select the best for the present problem. In particular, in the developed methodology, surrogate models are used to generate the row vector for any required parameter case and pre-multiplication of the basis leads to the necessary time history. Validation was performed considering the Mean Absolute Percentage Error (MAPE) in terms of the maximum/minimum IQs: the absolute percentage error is calculated considering the actual and the emulated results at the validation points and averaged for all the validation cases. A maximum MAPE of 8% is fixed to check the accuracy; if such desired level of accuracy is not met, then possible solutions to improve the results are:

1. increase the number of test samples keeping the same variation in the parameters
2. decrease the range of the input parameters, or
3. decrease the number of parameters for which the prediction is required.

C Uncertainty Quantification

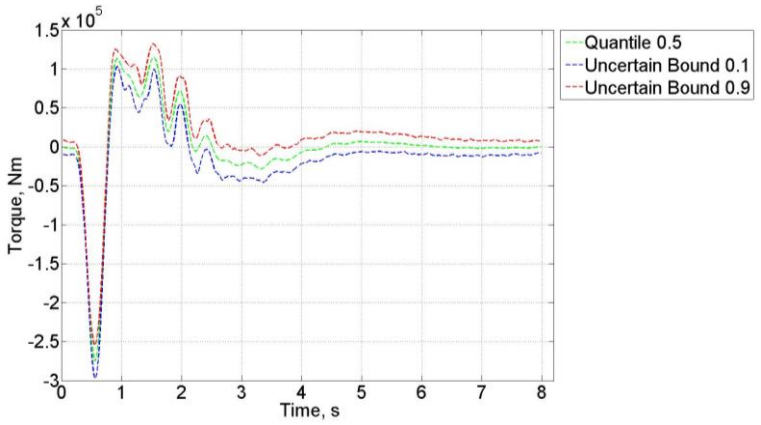

Figure 7. Example of a time histories (Torque) obtained for quantiles to 0.1, 0.5 and 0.9 directly

This methodology can be used to quantify the effects of uncertainty in the system parameters. Whereas for the 1D case the variation of the maximum and minimum IQ values can be easily tracked[1], the correlated time histories still need to be retained for each IQ. Using the reduced order surrogate model, it is possible to efficiently generate uncertainty bounds for the 1D time histories and the 2D correlated IQs plots by considering the quantiles of the IQs at each time instant. Although the uncertainty quantiles of each element of the rows of $\boldsymbol{U_k}$ can easily be found, it is not possible to then obtain physically-meaningful quantiles for the time history simply by multiplying the fixed basis $\boldsymbol{\Sigma_k V_k^T}$ by the determined quantile row vector of the coefficient $\boldsymbol{U_k}$ as the signs in the basis terms are not all positive. The quantiles of the IQs related to a specific time instant must be computed instead, in this case using the Kriging Method. Through adopting such an approach, the quantiles of the IQ time histories can be determined, and Fig. 7 shows typical trends for the 0.1, 0.5 and 0.9 quantiles. Note that the critical parameter case for each point on the quantile time histories is still maintained.

A more sophisticated approach needs to be used in order to determine the bounds of the convex hull of the correlated loads plots, ensuring that the correlation between the time histories of the individual IQs is maintained and also identifying which are the cases that lead to the critical correlated IQs. Taking the selected quantile bounds (q) as 0.1 and 0.9 as an example, it is not valid to simply plot the corresponding q = 0.1 and q = 0.9 quantile trends together, instead, all four possible combinations of correlated time histories between the q = 0.1 and q = 0.9 quantiles need to be plotted i.e. [IQ1(q=0.1) vs IQ2(q=0.1), IQ1(q=0.1) vs IQ2(q=0.9), IQ1(q=0.9) vs IQ2(q=0.1), IQ1(q=0.9) vs IQ2(q=0.9)].

For each quartet of points related to a specific time instant defines a rectangle in the 2D space that includes all the possible correlated IQs that can occurs at that instant, providing the required range of quantile-bounds within the defined rectangle. Typical correlated load plots for these combinations are shown in Fig. 8 and it can be seen that, in this particular case study, the plot identified by points with the different quantile in terms of the Bending Moment are almost the same. This behaviour is due to the fact that the bending modes are less sensitive to the gust loads and the varied structural parameters than the torsional modes. In order to determine the overall quantile bounds, the outer curve is found using a convex hull on all the four quantile time history combinations. The inner curve exploits the fact that quantile plots always intersect, and given m points belonging to n intersecting closed convex curves C, the inner bound of such curves is the locus of i≤m points that are inside n-1 curves C (the equality occurs only for n - overlapping curves). The inner bound identified in such a way cannot be convex.

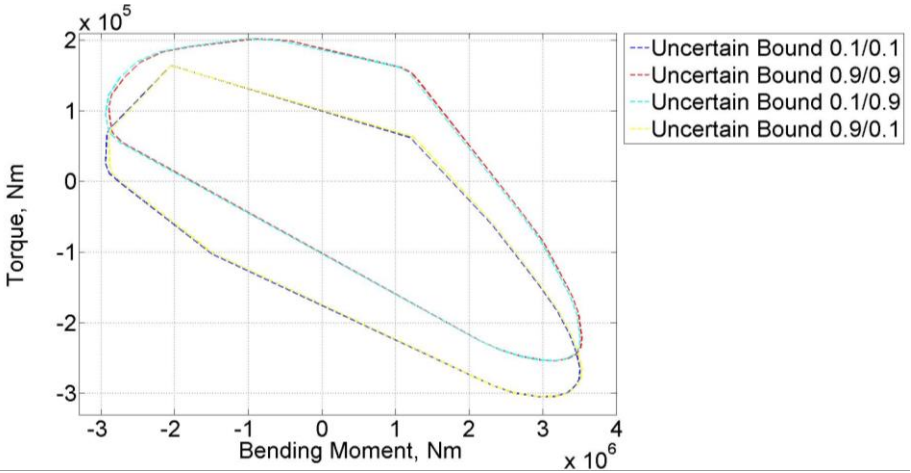

Figure 8. Potato plot for two IQs and four different quantile combinations. The legend provides the quantiles considered to obtain each convex hull in the format x-axis/y-axis IQ

Finally, in order to validate the UQ, the results have been compared with those obtained running directly the numerical model, i.e. operating a Monte Carlo Simulation (MCS), and considered as "truth". In particular, a maximum absolute percentage error of 8% is fixed for the maximum/minimum IQs.

IV. Results

Results using the methodologies discussed above were obtained for the time history simulations for the wing/engine system. Initially, only variations in the mass of engine and the stiffness of pylon (in terms of Young Modulus) were considered, and then the complexity was been increased to vary five parameters: the mass of the wings, wing flexural and torsional stiffness, and the engine mass and pylon stiffness. These cases are referred to as the 2D and 5D problems respectively. Table 4 shows the mean and the range adopted for the values of the structural parameters. In particular, the values assumed for the mass of Engine and the Young Modulus of the Pylon have been selected in according to the information provided by Manan.A et al.[8] and S. K. Choi[33]; the mean of the inertia moments, the structure and unstructured mass of the considered 10 stations along the wing are provided in the Appendix.

	Mean	Minimum	Maximum			Mean	Minimum	Maximum
Mass of Engine	8694.93 kg	-10%	+10%		m_f	-	-40%	+40%
Young Modulus	$69 \cdot 10^9$ Pa	-20%	+20%		**I**	-	-25%	+25%
					J	-	-25%	+25%

Table 4. Range of Variation of the structural parameters

A Singular Value Decomposition

Both 2D and 5D sampling planes for the surrogate training were considered in order to demonstrate how the accuracy increases in terms of the dimension of the sampling plane. Table 5 shows the number of samples that were considered and whether the z-score normalization was used; the adoption of a normalization approach and the number of Singular Values chosen depend upon the MAPEs discussed in Section 3.2. The aim was to capture those values that are significant to predict the behaviour of the convex hull even in presence of uncertainty in the input parameters.

	2D problem		**5D problem**	
Training Points	100	240	600	1000
Validating Points	30	30+100	150	150
Singular Values:				
Bending Moment	1	1	30	30
Torque	22	30	50	50
Zscore Norm	YES	YES	NO	NO

Table 5. Adopted Sampling Plane and SVs

B Surrogate Model: Training and Validation

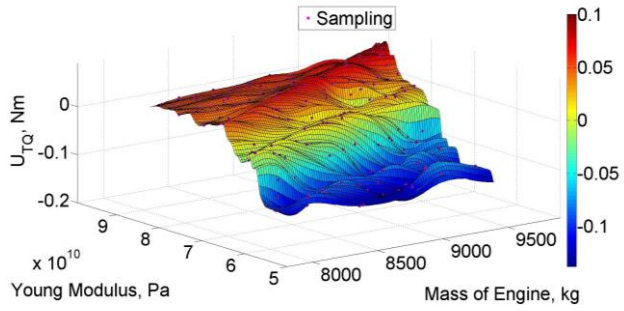

Figure 9. Example of a Surrogate Model obtained in the 2D problem using the *Blind Kriging method* for the first coefficient related to the torque.

The surrogate models presented in Section 3.2 were implemented: *Neural Networks*, *Tree*, *Polynomial Radial Basis Functions* and *Kriging*. In particular, among the *Kriging* Methods the *Ordinary* and *Blind Kriging* have been considered. With the only exception of the *Polynomial Radial Basis Function*, all the modes were constructed by considering a unit cube normalization for both the inputs and the outputs.

Figure 9 shows an example of a Surrogate Model of the first coefficient related to the Torque responses obtained in the 2D problem with 100 training points, whilst in Fig. 10 the "potato" plots predicted adopting surrogate models, always trained with 100 points, are compared to the one obtained running directly the numerical model (labelled with 'No Reduction'). After having trained the surrogate models and discarded those with a low accuracy, the validation step was accomplished and the MAPE evaluations discussed in Section 3.2 showed that the most accurate prediction for the correlated loads envelope was obtained using the Blind Kriging method (Fig. 11), which always provides the smallest MAPEs.

The key findings from the validation for both the 2D and 5D problems using the MAPEs show:

- best accuracy was achieved with the Blind Kriging surrogate model, in particular the evaluated MAPEs (Section 3) is always less than 0.1% for all the considered stations.
- predictors for bending moment were more accurate than the ones developed for the torque, which is due to the higher influence of the gust on the torsional modes.
- a slight improvement of the prediction if a higher number of training points is adopted.

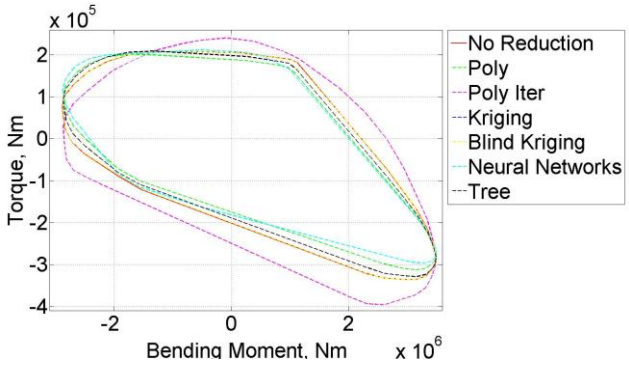

Figure 10. Reconstructed Correlated Load Plots using Different Surrogate Models.

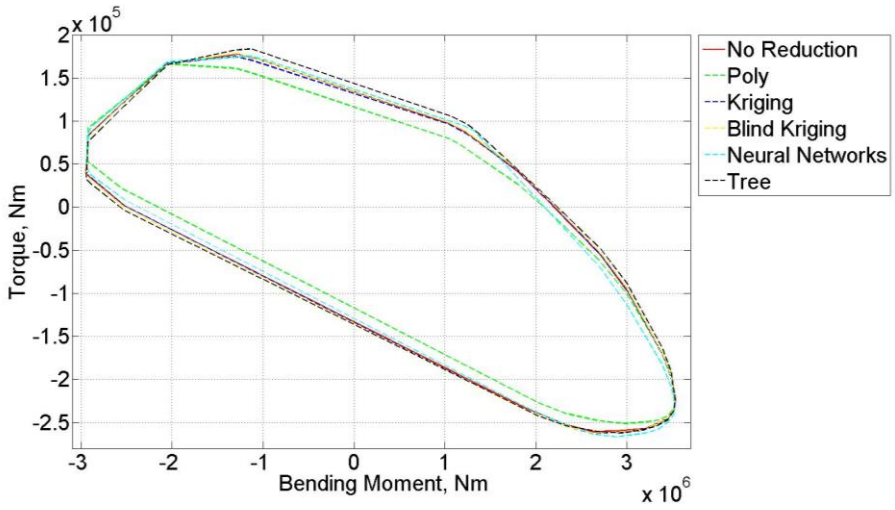

Figure 11. Validation in terms of Correlated Load Plots.

C Uncertainty Quantification

Results for the UQ are presented using the two different computations shown in Table 6. As already stated in section 3.3, the Monte Carlo Simulation (MCS) is included to provide a comparison for the ROM approach.

The methods for the *uncertainty propagation* presented in section V were applied to the 2D problem, considering the effects of uncertainty in the Engine mass and stiffness of the pylon, and the Kriging surrogate models trained with 100 points. The PDFs of such structural parameters have been assumed to be Gaussian and the main statistical quantities[8] are summarized in table 7.

	Case	
	1	2
Quantiles	Forces	Forces
Method	SVD + Kriging	MCS

Table 6 Cases compared in section 6 for the UQ.

	Mean μ	**COV**	**σ**
Mass of Engine	8694.93 kg	0.039	339.1 kg
Young Modulus of the Pylon	$69 \cdot 10^9$ Pa	0.1	$69 \cdot 10^8$ Pa

Table 7 Adopted statistical quantities.

First of all it is important to underline that once the time history related to the desired quantiles are determined, the *behaviour of the convex*, the *correlated*

[8] A sub-domain of the uncertain inputs is considered (Table 6). These subdomains capture 98.97% and 95.45% of the probability distribution for the mass of engine and stiffness of pylon, respectively.

loads at different stations at the same critical case load, the *critical case loads and relative instants* for all the desired stations can be detected with simply mathematical considerations. In this regard, Fig. 12 shows the critical load cases, which are expressed in terms of the lengths of gust (L_g), characterizing the bounds of the convex hull and the "potato" plot detected fixing 0.5 quantile for both the IQs. In particular, they are obtained at the wing root using the SVD-based method together with Blind Kriging Surrogate Models.

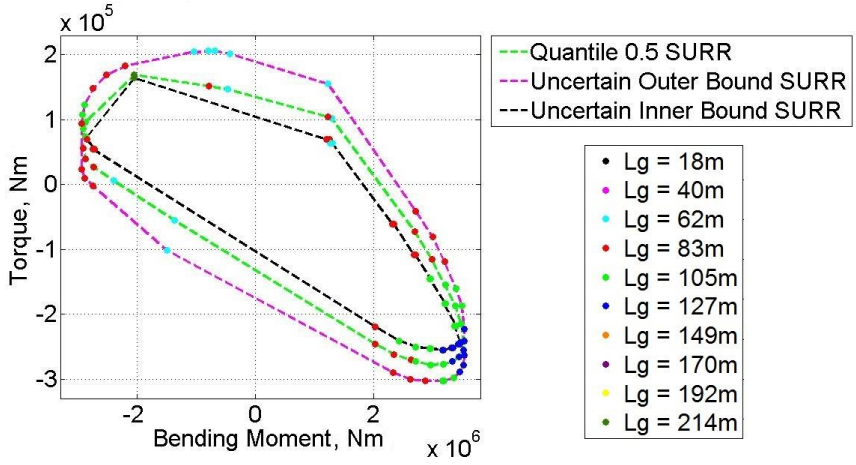

Figure 12. UQ obtained applying the SVD-based method together with the Blind Kriging model. The colored points on the bounds stand for the critical ones.

1. Comparison of UQ SVD-based methods

In order to validate the UQ, a Monte Carlo Simulation was conducted for the 2D problem and considered as the "truth". The numerical model was run 1200 times and the IQs post-processed in order to determine the sought quantiles. The surrogate model has been emulated 600, 1200 and 2400 times to check if differences in the results would occur. In all the three cases, the estimated quantiles are practically the same and the results are satisfactory, i.e. fulfilled the required accuracy (Section 3.3). There is only a slightly improvement adopting the last two. Thus, the results obtained considering 1200 emulations for the surrogate model are presented here.

Figure 13 shows a comparison of bounds of convex hull and the "potato" plot detected fixing 0.5 quantiles for both the IQs at three stations: at wing root, just inboard of the engine and at the wing tip. In all the cases very good agreement is obtained.

In order to complete the proof of goodness of the developed method, percentage errors obtained emulating the *Blind Kriging* surrogate model rather than evaluating MCSs of the numerical model are considered for a set of quantiles. Table 8 shows the maximum of the absolute-percentage errors of the maximum/minimum IQs, and for which quantile they are obtained, for all the stations along the wing.

Even in the presence of some errors, it has been demonstrated, by comparing the convex hulls and their critical lengths, that the required accuracy is excellent. Indeed, we have verified that adopting the developed method for the UQ the required critical conditions for the aircraft are identified with very good accuracy: the *correlated loads* at different stations at the same critical case load and the *critical case loads* for all the desired stations are the same of those obtained adopting the MCS technique.

Moreover, the developed method requires much less computation than MCS computational cost; for the 2D study considered, using a desktop PC, a MCS takes about 2 days to propagate the uncertainty, whereas the developed methods requires about 2 hours both to train all the surrogate models and propagate the uncertainty up to the convex hull.

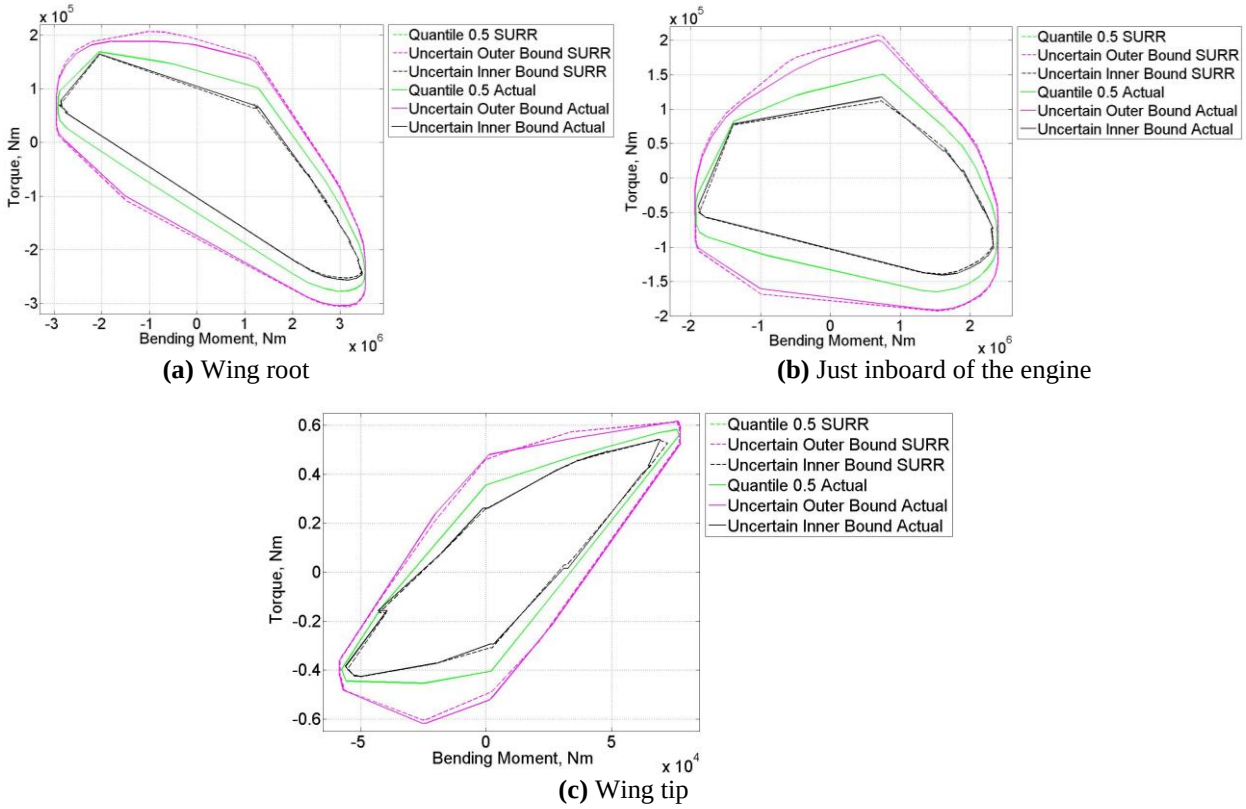

(a) Wing root

(b) Just inboard of the engine

(c) Wing tip

Figure 13. Validation of the UQs. Comparison of convex hulls obtained at three stations for a 10 1MC gust family using the emulation of the developed Blind Kriging surrogate model (SURR) and a MCS of the numerical model (Actual).

	Station									
	1	**2**	**3**	**4**	**5**	**6**	**7**	**8**	**9**	**10**
	Percentage Error Maximum Bending Moment									
Value	0.099 %	0.046%	0.23%	0.29%	0.29%	0.3%	0.32%	0.36%	0.53%	0.86%
Quantile	0.3	0.3	0.7	0.9	0.9	0.9	0.9	0.9	0.1	0.1
	Percentage Error Minimum Bending Moment									
Value	0.34%	0.14%	0.45%	0.23%	0.24%	0.25%	0.28%	0.62%	0.64%	0.57%
Quantile	0.7	0.1	0.9	0.9	0.9	0.9	0.8	0.9	0.9	0.9
	Percentage Error Maximum Torque									
Value	6.8%	7.2%	6.9%	0.62%	0.48%	0.43%	0.22%	0.16%	0.37%	1.4%
Quantile	0.9	0.9	0.5	0.1	0.1	0.1	0.1	0.1	0.9	0.3
	Percentage Error Minimum Torque									
Value	1.2%	1.3%	1.9%	0.35%	0.37%	0.21%	0.13%	0.11%	0.17%	7.8%
Quantile	0.9	0.9	0.5	0.1	0.9	0.9	0.2	0.2	0.1	0.4

Table 8 Maximum of the absolute-percentage errors with respect to the MCS for the maximum/minimum IQs for each station and quantiles. The considered quantiles are from 0 to 1 with an increment of 0.1.

V. Conclusions and Further Work

A SVD-based method for both the prediction and the propagation of the uncertainty in terms of correlated aircraft loads has been presented and has been validated considering an aeroelastic model of a civil aircraft. For both the prediction and the UQ, the Blind Kriging surrogate model gave the most accurate results and good quality predictions were obtained considering variations for both two (2D) and five (5D) structural parameter variations. It has been shown that using the SVD together with the Blind Kriging surrogate model, all the required information related to the behaviour of the "potato" plots, the correlated IQs and the critical conditions can be captured. Very good results have been achieved for the prediction of correlated loads, and the comparison between the results obtained for the uncertainty quantification, using the developed method and Monte Carlo Simulation, showed an excellent agreement with a significant reduction (approximately 95%) in computation.

The SVD-based method can be simply generalized for higher dimensions, once suitable surrogate models of the coefficients have been determined.

Future work will improve the application of the developed techniques, investigating the application to a more complex aircraft model, considering more configurations/conditions and design parameters, the inclusion of nonlinear effects, and the use of piecewise Gaussian processes for the uncertainty quantification.

Appendix

A Structural Parameters along the wing

Table 9 and 10 show the nominal values for the inertia moments (I and J), the structured (CONM2) and nonstructural mass (nstrM) of the 10 stations considered along each wing.

Element	**I** (m^4)	**J** (m^4)	**nstrM** (kg/m)
1	$2.12 \cdot 10^{-2}$	$7.78 \cdot 10^{-2}$	2122
2	$1.48 \cdot 10^{-2}$	$5.4 \cdot 10^{-2}$	1618
3	$9.97 \cdot 10^{-3}$	$3.63 \cdot 10^{-2}$	1258
4	$7.13 \cdot 10^{-3}$	$2.59 \cdot 10^{-2}$	1017
5	$5.19 \cdot 10^{-3}$	$1.88 \cdot 10^{-2}$	805.9
6	$3.38 \cdot 10^{-3}$	$1.22 \cdot 10^{-2}$	619.1
7	$1.8 \cdot 10^{-3}$	$6.52 \cdot 10^{-3}$	66.32
8	$5.21 \cdot 10^{-4}$	$1.92 \cdot 10^{-3}$	52.03
9	$3.45 \cdot 10^{-5}$	$1.32 \cdot 10^{-4}$	34.63

Table 9. Nominal values of the inertia moments ad nonstructural mass.

Station	**CONM2** (kg)
1	666.1
2	881.8
3	665.8
4	515.5
5	408.3
6	314.8
7	233.5
8	183.5
9	131.2
10	56.08

Table 10. Nominal values of the structured mass.

Acknowledgments

This work is supported by the European Commission (EC FP7) under the Marie Curie European Industrial Doctorate Training Network 'ALPES' (Aircraft Loads Prediction using Enhanced Simulation) and also the Royal Academy of Engineering.

References

[1]J. R. Wright & J.E. Cooper, "Introduction to Aircraft Aeroelasticity and Loads", Wiley, 2007.

[2]FM Hoblit, "Gust Loads on Aircraft – Concepts and Applications", AIAA, 1988.

[3]TL Lomax, "Structural Loads Analysis for Commercial Transport Aircraft: Theory and Practice", AIAA Education Series 1999.

[4]H.H. Khodaparast, G. Georgiou, J.E. Cooper, L. Travaglini, S. Ricci, G.A. Vio & P. Denner "Rapid Prediction of Worst Case Gust Loads", J.Aeroelasticity and Structural Dynamics. v2 n3 2012.

[5]H.H. Khodaparast, G. Georgiou, J.E. Cooper, L. Travaglini, S. Ricci, G.A. Vio & P. Denner "Efficient Worst Case '1 – Cosine' Gust Loads Prediction", IFASD 2011 Paris, France.

[6]H.H. Khodaparast and J.E. Cooper "Rapid Prediction of Worst Case Gust Loads Following Structural Modification" AIAA Journal, 2014 v52, n2 pp 242-254.

[7]H.H. Khodaparast, J.E. Cooper, L. Cavagna, S. Ricci and L. Riccobene. "Fast Prediction of Worst Case Gust Loads" International Forum on Aeroelasticity and Structural Dynamics, 2013.

[8]S. K. Choi, R. V. Grandi, R. A. Canfield "Reliability-based Structural Design", Springer-Verlag London Limited 2010.

[9]D. Xiu and G. E. Karniadakis, "The Wiener-Askey Polynomial Chaos for Stochastic Differential Equations", in Society for Industrial and Applied Mathematics Journal on Scientific Computing (SIAM J.Sci), 2002, Vol.24, No. 2 pp. 619-644.

[10]M. S. Eldred "Recent Advances in non-Intrusive Polynomial Chaos and Stochastic Collocation Methods for Uncertainty Analysis and Design", in 50th AIAA/ASME/ASCE/AHS/ASC Structures, Structural Dynamics, and Material Conference, 4-7 May 2009, Palm Springs, California.

[11]G. Georgiou, A. Manan & J.E. Cooper, "Modeling Composite Wing Aeroelastic Behaviour with Uncertain Damage Severity and Material Properties" Mechanical Systems and Signal Processing, Vol 32, October, 2012, pp. 32-43.

[12]K.J. Badcock, H.H. Khodaparast, S. Timme, and J.E. Mottershead, "Calculating the Influence of Structural Uncertainty on Aeroelastic Limit Cycle Response'', 52nd AIAA/ASME/ASCE/AHS/ASC Structures, Structural Dynamics, and Materials Conference, Denver, Colorado, 4-8 Apr. 2011.

[13]C. Scarth, J.E. Cooper, P. M. Weaver, G. H.C. Silva "Uncertainty Quantification of Aeroelastic Stability of Composite Plate Wings using Lamination Parameters" Composite Structures 2014 v116 pp 84-93.

[14]S. K. Choi, R. V. Grandhi, R. A. Canfield & C. L. Pettit "Polynomial Chaos Expansion with Latin Hypercube Sampling for Estimating Response Variability", AIAA Journal, Vol. 42, No. 6, June 2004.

[15]C. L. Pettit "Uncertainty Quantification in Aeroelasticity: Recent Results and Research Challenges", in Journal of Aircraft, Voll.41, No. 5, September-October 2004.

[16]Q. Ouyang, X. Chen & J. E. Cooper, "Robust Aeroelastic Analysis and Optimization of Composite Wing Under μ-Analysis Framework", J.Aircraft Vol. 50, 2013, pp. 1299-1305.

[17]E. Albano & W.P. Rodden, "A Doublet-Lattice Method for Calculating Lift Distributions on Oscillating Surfaces in Subsonic Flows" AIAA J. Vol. 7 n2 pp 279-285, 1969.

[18]TITLE 14, Aeronautics and Space, Part 25, Airworthiness Standards: Transport Category Airplanes, Subpart C, Structure, Flight Maneuver and Gust Conditions. (§25.333 Flight maneuvering envelope, §25.341 Gust and turbulence loads), November 6, 2014.

[19]K. Worden, W. J. Staszewski, J. J. Hensman, "Natural Computing for Mechanical Systems Research: A Tutorial Overview", Mechanical Systems and Signal Processing, Volume 25, Issue 1, January 2011, Pages 4-111.

[20]J. C. Helton and F.J. Davis, "Sampling-Based Methods for Uncertainty and Sensitivity Analysis", SAND99-2240, Albuquerque, NM, Sandia National Laboratories, July 2000.

[21]A. Manan & J.E. Cooper J.E. "Design of Composite Wings Including Uncertainties – A Probabilistic Approach", J.Aircraft. v46n2 2009 pp601-607.

[22]G.H. Golub & C.F. Van Loan "Matrix Computations", 2nd ed. John Hopkins Press 1989.

[23]S. Sarkar, A. Dong, J. S. Gero, "Design Optimization Problem Reformulation using Singular Value Decomposition", Journal of Mechanical Design, 2009.

[24]S. McGuinness, C. G. Armstrong, A. Murphy, J. Barron, M. Hockenhull, "Improving Aircraft Stress-Loads Evaluation and Optimization Procedures", 2nd Aircraft Structural Design Conference, London, United Kingdom, 2010.

[25]A. Forrester, A. Sóbester, A. Keane "Engineering Design via Surrogate Modelling: a practical guide", Chichester, UK, Wiley, 2008.

[26]I. Couckuyt, T. Dhaene, P. Demeester "ooDACE toolbox, A Matlab Kriging toolbox: Getting started", 3rd June 2013.

[27]V. R. Joseph, Y. Hung, A. Sudjianto "Blind Kriging: A New method for Developing Surrogate models", Journal of Mechanical Design, Vol. 130, Issue 3, Research Paper, February 04, 2008.

[28]I. Couckuyt, A. Forrester, D. Gorissen, F. De Turck, T. Dhaene "Blind Kriging: Implementation and performance analysis", Advances in Engineering Software, Vol. 49, pp. 1-13, July 2012.

[29]I. Couckuyt, F. Declercq T. Dhaene, H. Rogier, L. Knockaert "Surrogate-based infill optimization applied to electromagnetic problems", Special Issue on Advances in Design Optimization of Microwave/RF Circuits and Systems, Vol. 20, No. 5, pp. 492-501, September 2010.

[30]G. Georgiou, H. H. Khodaparast, J. E. Cooper "Uncertainty Quantification of Aeroelastic Stability", Mathematics of Uncertainty Modeling in the Analysis of Engineering and Science Problems, IGI global, 2014, pp.329-356.

[31]J. D. Martin, T. W. Simpson "On the use of Kriging Models to approximate deterministic computer models", in Proceedings of DETC'04: ASME 2004 International Design Engineering Technical Conference and Computer and Information in Engineering Conference, Salt Lake City, Utah USA, September 28 – October 2, 2004.

[32]StatSoft, Inc. (2013). Electronic Statistics Textbook. Tulsa, OK: StatSoft. WEB: http://www.statsoft.com/textbook/.

[33]M.T. Tong, "A Probabilistic Approach to Aeropropulsion System Assessment", NASA Technical Reports Server NASA/TM-2000-210334, Glenn Research Center, Cleveland, Ohio, USA.